PNL-4001-2
UC-90g

Development of Materials for Open Cycle MHD

Quarterly Report for the Period Ending December 1982

D. D. Marchant
J. L. Bates

March 1983

Prepared for the U.S. Department of Energy
under Contract DE-AC06-76RLO 1830

Pacific Northwest Laboratory
Operated for the U.S. Department of Energy
by Battelle Memorial Institute

Battelle

PNL-4001-2

DISCLAIMER

PACIFIC NORTHWEST LABORATORY
operated by
BATTELLE
for the
UNITED STATES DEPARTMENT OF ENERGY
under Contract DE-AC06-76RLO 1830

Printed in the United States of America
Available from
National Technical Information Service
United States Department of Commerce
5285 Port Royal Road
Springfield, Virginia 22151

NTIS Price Codes
Microfiche A01

Printed Copy

Pages	Price Codes
001-025	A02
026-050	A03
051-075	A04
076-100	A05
101-125	A06
126-150	A07
151-175	A08
176-200	A09
201-225	A010
226-250	A011
251-275	A012
276-300	A013

PNL-4001-2
UC-90g

DEVELOPMENT OF MATERIALS FOR OPEN CYCLE MHD

Quarterly Report for the Period
Ending December 1982

D. D. Marchant
J. L. Bates

March 1983

Prepared for the
U.S. Department of Energy
under Contract DE-AC06-76RLO 1830

Pacific Northwest Laboratory
Richland, Washington 99352

SUMMARY

Pacific Northwest Laboratory (PNL) is conducting an ongoing study of channel components for open cycle, coal-fired magnetohydrodynamic generators. Specifically, electrodes/insulators are being developed and tested. For this study, a hot-walled test channel with eight electrodes was fabricated for testing in the WESTF test facility at Westinghouse Research and Development Laboratory, Pittsburgh, Pennsylvania. The channel is designed to operate hot on all four walls, thereby reducing the amount of condensed slag. The compositions of four of the electrodes in the test channel were based on hafnium oxide-rare earth oxides-indium oxide.

The electrical conductivity has been measured on several compositions based on hafnium oxide-rare earth oxides-indium oxides. The results show that adequate conductivity may be obtained with reduced indium oxide content as long as praseodymium oxide is used as the rare earth.

CONTENTS

INTRODUCTION

Pacific Northwest Laboratory (PNL) is developing and testing ceramic electrodes/insulators and other channel components for open cycle, coal-fired magnetohydrodynamic (MHD) generators as part of the Department of Energy's Power Generation Programs. The PNL program is divided into four tasks:

- Development and Fabrication of Electrodes/Insulators
- Design and Testing of Electrodes/Insulators
- Characterization and Evaluation of Electrode/Insulator Materials
- Thermal, Electrical, and Mechanical Property Measurement.

The objectives of the program are as follows:

1. develop electrodes that can withstand the severe corrosive and erosive environment of an MHD channel and that will transfer electrical current efficiently during long channel operation
2. develop insulators that can withstand the corrosive and erosive environment and maintain adequate electrical resistivity during long channel operation
3. develop electrode and insulator designs that are compatible with the demands of channel assembly, operation, and disassembly.

Because all of the tasks are interrelated, the quarterly reports are organized by activities and not necessarily by specific tasks. This report summarizes two activities: the design and fabrication of a channel for testing in the WESTF MHD test facility[a] and the development of highly conducting ceramic oxides for electrode current leadouts.

(a) Operated by Westinghouse Research and Development Laboratory, Pittsburgh, Pennsylvania.

TECHNICAL PROGRESS

An MHD test channel was designed and assembled at PNL for testing in the WESTF facility. The channel was delivered in September 1982; the tests have not yet been conducted. The following subsection discusses the design and assembly of the test channel.

Work on the ceramic oxide electrodes is ongoing. The second subsection reports progress to date on the development of current leadout materials for the electrodes.

DESIGN AND ASSEMBLY OF AN MHD TEST CHANNEL

The purpose of the WESTF test is to determine the electrical and thermal characteristics of ceramic superhot electrodes surrounded by a metal fin; verify the electrode design parameters; and determine the thermomechanical performance and the extent of corrosion/erosion of the electrodes in an electric field when exposed to the slag, potassium seed, and sulfur-containing MHD environment.

The test channel consists of eight electrodes (four anodes and four cathodes) with interelectrode refractory ceramic oxide insulators and refractory ceramic oxide side walls. The channel electrodes are instrumented with thermocouples to better define the thermal characteristics and determine the heat flow. The outside of the channel consists of a stainless steel jacket, supplied by Westinghouse, which contains water passages for cooling during the test. The jacket is of one piece construction with holes in two opposite sides for inserting the electrodes. The inside dimensions of the jacket are 7.6 cm by 6 cm. The length is 37.8 cm. The diameter of the holes used to insert the electrodes is 3.2 cm.

Because the channel was designed for hot wall operation, the jacket is lined on the inside with refractory ceramic oxide, which allows the inside surfaces to operate at temperatures above 1475K. The high temperatures are necessary to minimize the amount of slag that might condense from the plasma. Previous hot ceramic electrode tests generally used hot electrodes in a channel

with colder side walls or other areas; consequently, slag condensed on colder walls, then flowed over the hot electrodes and increased the corrosion of the electrodes.

The refractory ceramic oxide used to line the jacket is a fused cast magnesium oxide/magnesium oxide-aluminum oxide spinel (MMAS). The spinel, which is an experimental composition, was supplied by Applied Technology Laboratories[(a)] (Butte, Montana) and manufactured by Cohart (Louisville, Kentucky). The Cohart designation is X-317. The density of the MMAS is 3.37 g/cm^3 with an open porosity of 2 vol%. The microstructure consists of magnesium oxide crystals within a matrix of spinel solid solution (Bates and Marchant 1982a). The average thickness of the spinel is 12.1 mm, covering both the electrode and side walls. The dimensions of the channel after lining are 3.6 cm by 52.1 cm; 3.6 cm is the distance between the electrodes.

Originally in the form of bricks approximately 7.6 cm x 7.6 cm x 43 cm, the MMAS was cut to the shapes required for the channel. The centers of the bricks were porous due to the fuse casting process, so only the material near the outside of the brick could be used for the channel. The spinel lengths varied between 10 and 18 cm. Three spinel pieces were required to line each wall. The joints between the pieces were rabbited to eliminate direct pathways between the plasma and the stainless steel jacket. The rabbitting also helped to produce interlocking joints for mechanically holding the MMAS pieces together.

The spinel was attached to the stainless steel walls by a heat-curable, silicone rubber adhesive (75 U, Dow Corning, Midland, Michigan). Before the adhesive was applied, the ceramic and stainless steel surfaces were cleaned with successive washes of trichlorethylene and acetone, then coated with a primer (1300, Dow Corning, Midland, Michigan). The adhesive was flattened into sheets about 0.018 cm thick and placed between the spinel and the channel. The adhesive was cured by heating to 427K for 30 min in an oven. The post-cure

(a) Use of manufacturer names does not imply PNL endorsement.

treatment consisted of heating to 449K for 4 h. A silicone rubber insert placed inside the lined channel helped to hold the ceramic in place during curing.

Since the jacket one piece, the ceramic linings had to be slipped in from the ends. The silicone adhesive was placed on the spinel, and the spinel was slipped into the channel. Unfortunately, the spinel cracked in some places in the neck between the electrodes while it was being put into the channel. However, these cracks will not be detrimental to the operation of the channel.

The eight electrodes (four anodes and four cathodes) were mounted in the channel by inserting the electrode/insulator/water-cooling assembly (Figure 1) through holes in the jacket. The design is similar to that reported for the AVCO tests (Marchant and Bates 1982a) except a circular geometry was used. The electrode consists of a cylindrical sintered ceramic body surrounded by a copper sleeve. The back face of the ceramic is in contact with copper metal mesh with a theoretical density near 50%, which is attached to a copper water-cooling assembly. The copper sleeves were brazed to the cooling assembly with a braze containing 30 wt% Ag, 20 wt% Cd, 27 wt% Cu, and 23 wt% Zn (Easy-Flo 30, Handy and Harmon, New York). The braze liquidus was 983K and the solidus 878K. The brazing flux was WELCO Flux 250 (Welco Alloys, Madison Heights, Michigan). The brazing was done in air using a propane and air flame. An RTV silicone rubber (RTV 106, General Electric, Waterford, New York), containing 5 wt% natural flake graphite, was used as the electrically conducting, flexible adhesive connecting the copper sleeve, copper mesh, and ceramic. This rubber has a maximum useful temperature of 573K.

The electrode compositions are listed in Table 1. The two electrodes based on hafnium oxide (positions 1 and 4) are composites containing a cap and a current leadout. The cap is in contact with the hot MHD plasma. The cap is refractory and is of a composition to resist high-temperature corrosion. The electrical conductivity of the cap is only adequate at elevated temperatures. The current leadout is located between the cap and the copper mesh. The leadout is not as refractory or as corrosion resistant as the cap but has adequate

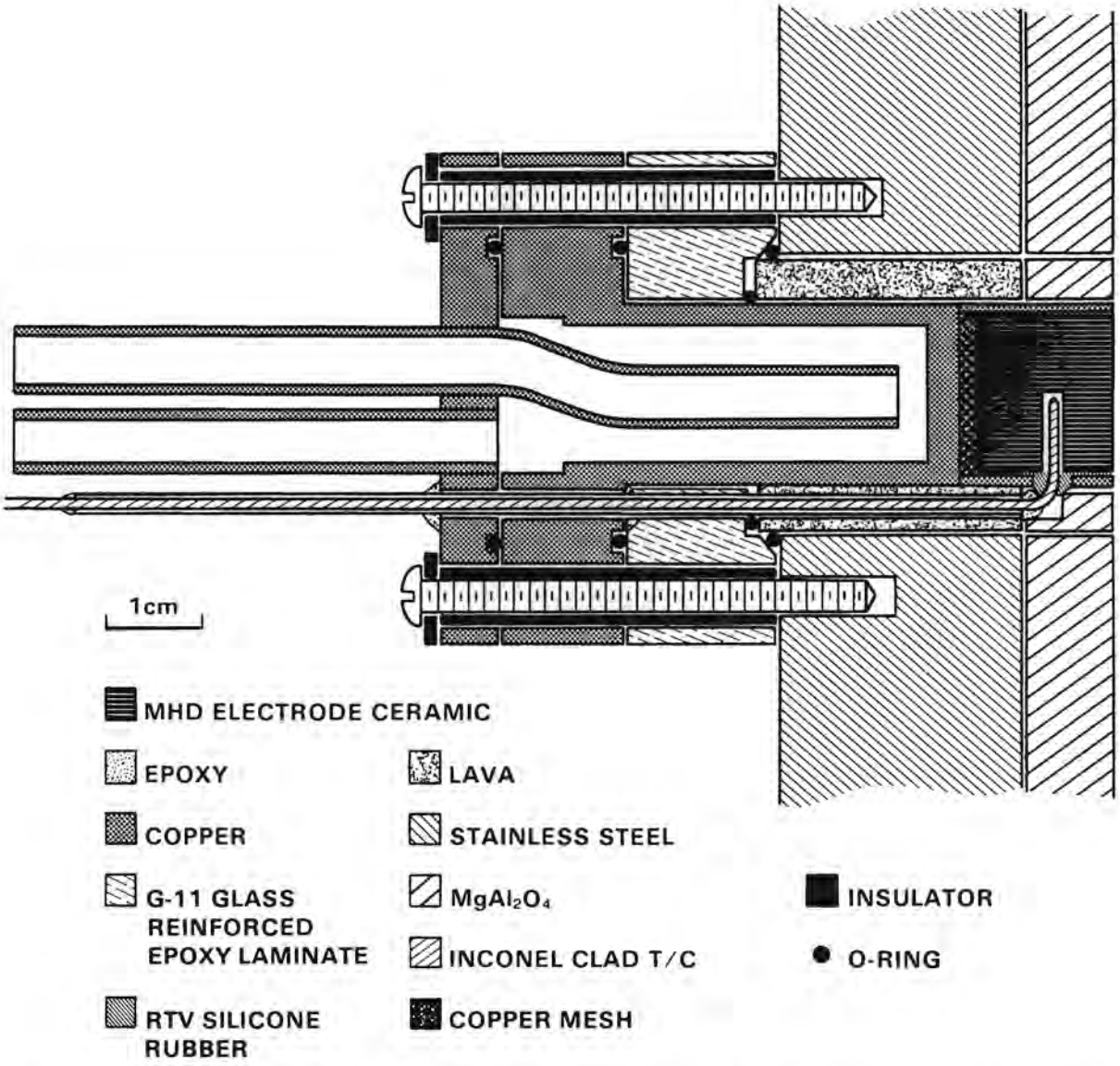

FIGURE 1. Cross Section of Electrode/Insulator and Water-Cooling Assembly

electrical conductivity to room temperature. The cap andcurrent leadout are of monolithic construction and were fabricated by sintering as an integral body from reactive powders.

The two electrodes based on yttrium chromite (Table 1) are of one composition throughout since the electrical conductivity is adequate over the temperature range of operation. Because the chromite materials are not as

TABLE 1. Electrodes for WESTF Test

Electrode Position	Electrode Composition, mol%	Material Thickness, cm	Thermocouple		Copper Ring Thickness, cm
			Anode	Cathode	
1 (Cap)	$6.8Y_2O_3 \cdot 93.2HfO_2$	0.28	Yes	No	0.10
(Leadout)	$62.5In_2O_3 \cdot 2.1Pr_6O_{11} \cdot 2.9Yb_2O_3 \cdot 32.3HfO_2$	1.14			
2	$Y(Ca_{0.05}Cr_{0.95})O_3$	1.42	No	Yes	0.10
3	$Y(Mg_{0.05}Cr_{0.95})O_3$	1.42	Yes	No	0.14
4 (Cap)	$7.9Pr_6O_{11} \cdot 3.8Yb_2O_3 \cdot 88.3HfO_2$	0.28	Yes	No[a]	0.10
(Leadout)	$62.5In_2O_3 \cdot 2.3Pr_6O_{11} \cdot 2.9Yb_2O_3 \cdot 32.3HfO_2$	1.14			

(a) Optical sight port.

corrosion resistant at high temperatures as the hafnium oxide materials, the yttrium chromite electrodes are designed to operate at an electrode/plasma interface temperature about 150K less than for the hafnium-based materials.

Several electrodes contain an alumel-chromel thermocouple that is ungrounded to an Inconel 600 sheath (SCAIN-040U-6, Omega Engineering, Inc., Stamford, Connecticut). The Inconel sheath limits the useful temperature of thermocouple to 1422K. The center of the thermocouple hole is 0.76 cm from the electrode-channel surface. The depth of the thermocouple hole was designed so that the thermocouple tip is at the centerline of the electrode. The hole diameter is about 0.002 cm greater than the thermocouple (0.1 cm) to minimize the temperature difference between the electrode and thermocouple.

Inside the channel, the electrodes are electrically isolated by the spinel insulator (see Figure 1). An alumina-silica machinable ceramic was used between the copper cooling assembly and the stainless steel. The cooling copper flange was separated from the stainless steel by a fiberglass-filled epoxy. The brass bolts used to attach the stainless steel to the copper were surrounded by heat shrinkable tubing, with fiberglass-filled epoxy washers placed under the head. The hole in the copper used for the thermocouple and alumina tube was sealed with epoxy (Epoxi-Patch).

HIGHLY CONDUCTING OXIDE CURRENT LEADOUTS

Ternary oxides based on hafnium oxide-rare earth oxides-indium oxide (HfO_2-RE_xO_y-In_2O_3) are being developed at PNL as oxide current leadouts for high-temperature, MHD ceramic electrodes (Bates and Marchant 1982b,c). These oxides exhibit high electrical conduction (20 to 40 S/cm at 1000K), thermal stability in air to 1750K, and generally high resistance to electrochemical corrosion in molten potassium sulfate (K_2SO_4) and potassium carbonate (K_2CO_3) at current densities (~1 A/cm^2). Cursory studies show that certain rare earth oxide and indium oxide additions result in a pyrochlore structure that is highly electrically conducting. By changing the rare earth and indium oxide concentrations, the electrical conductivity, transport, and other electrical and structural properties can be modified significantly. However, only a narrow range of compositions have been studied and their properties measured.

Electrical conductivity and phase equilibria are being studied to emphasize those compositions that provide the best corrosion resistance to molten potassium seed and the highest electrical conductivity. Two general trends can be used as guides for selecting compositions for these studies.

- The compositions examined so far that have the highest electrical conductivity and lowest activation energies contain praseodymium oxide and indium oxide.
- Increases in indium tend to increase the electrical conductivity when large amounts of yttrium oxide and/or ytterbium oxide are not present. When significant amounts of these oxides are present, electrical conductivity decreases with increases in indium oxide.

Electrical Conductivity

The electrical conductivity of these highly conducting oxides is being measured to 1700K in air using a four-contact direct method. A square bar sample is positioned in an aluminum oxide (Al_2O_3) muffler furnace, using platinum knife edges as current and voltage probes positioned with Al_2O_3 hardware. All samples were prepared by the cold uniaxial and isostatic powder pressing of coprecipitated powders into a compact and sintering the compact in air at 1850K. The sintered densities were >90% TD. The resulting structures were examined by x-ray diffraction and found to contain different phases depending on the chemical compositions. The phases generally were cubic fluorite, cubic pyrochlore, monoclinic (usually unstabilized hafnium oxide), body centered cubic (like indium oxide), and the rare earth cubic structure.

A wide variation in conductivity, up to 8 orders of magnitude, occurs for the different compositions, as reported previously (Bates and Marchant 1982b). These data generally can be expressed as two linear equations with the intersection of the two lines from 800 to 900K, with the high-temperature data having a larger slope. The fit of the data is very good, with coefficients of determination better than 0.99 and 0.95 for the high and low temperatures, respectively.

The data can be separated into two groups. The group with the highest conductivities exhibit lower activation energies, i.e., 0.38 to 0.66 eV and 0.156 to 0.27 eV for the high and low temperatures, respectively. The group

with the lower conductivities have higher activation energies at high temperatures, 1.00 to 1.79 eV, but low-temperature energies are near 0.17 eV. Although a good correlation has not been developed, the conductivity appears to be partially related to the crystal structure along with the composition.

The effect of indium oxide concentration on electrical conductivity is of major interest to this study. To investigate this effect, the electrical conductivity of a nominal $0.06Pr_6O_{11}\cdot 0.87HfO_2\cdot 0.07Yb_2O_3$ base composition containing varied amounts of indium is being measured. This composition was selected because it has demonstrated the highest electrical conductivity when indium oxide is added, and has shown good corrosion resistance to molten K_2SO_4. However, it does contain both the fluorite and pyrochlore phases. The electrical conductivities are shown in Figure 2 with the compositions tabulated below.

AF-1	$0.85(0.06Pr_6O_{11}\cdot 0.87HfO_2\cdot 0.07Yb_2O_3)\cdot 0.15In_2O_3$
AG-1	$0.75(0.06Pr_6O_{11}\cdot 0.87HfO_2\cdot 0.07Yb_2O_3)\cdot 0.25In_2O_3$
LLL	$0.70(0.06Pr_6O_{11}\cdot 0.88HfO_2\cdot 0.06Yb_2O_3)\cdot 0.30In_2O_3$
AB-1	$0.43(0.06Pr_6O_{11}\cdot 0.87HfO_2\cdot 0.07Yb_2O_3)\cdot 0.57In_2O_3$
BB	$0.55(0.17Pr_6O_{11}\cdot 0.83HfO_2)\cdot 0.45In_2O_3$
KKK	$0.61(0.06Pr_6O_{11}\cdot 0.88HfO_2\cdot 0.06Yb_2O_3)\cdot 0.39In_2O_3$

The results suggest a sharp increase in electrical conductivity near 25 mol% In_2O_3, with much smaller increases above 30 mol% In_2O_3. The composition showing the higher electrical conductivity contain the pyrochlore phase. The lower conductivity contains cubic fluorites. Consequently, the formation of the pyrochlore structure for HfO_2-RE_xO_y as the base oxide appears to be a necessary requirement for high electrical conductivity. From the equilibrium phase relationships (Kravchinskaya et al. 1978), the range of compositions for the HfO_2-Pr_6O_{11} single-phase pyrochlore structure is 0.11 to 0.19 mol% Pr_6O_{11}. This range should therefore be studied as a function of indium content.

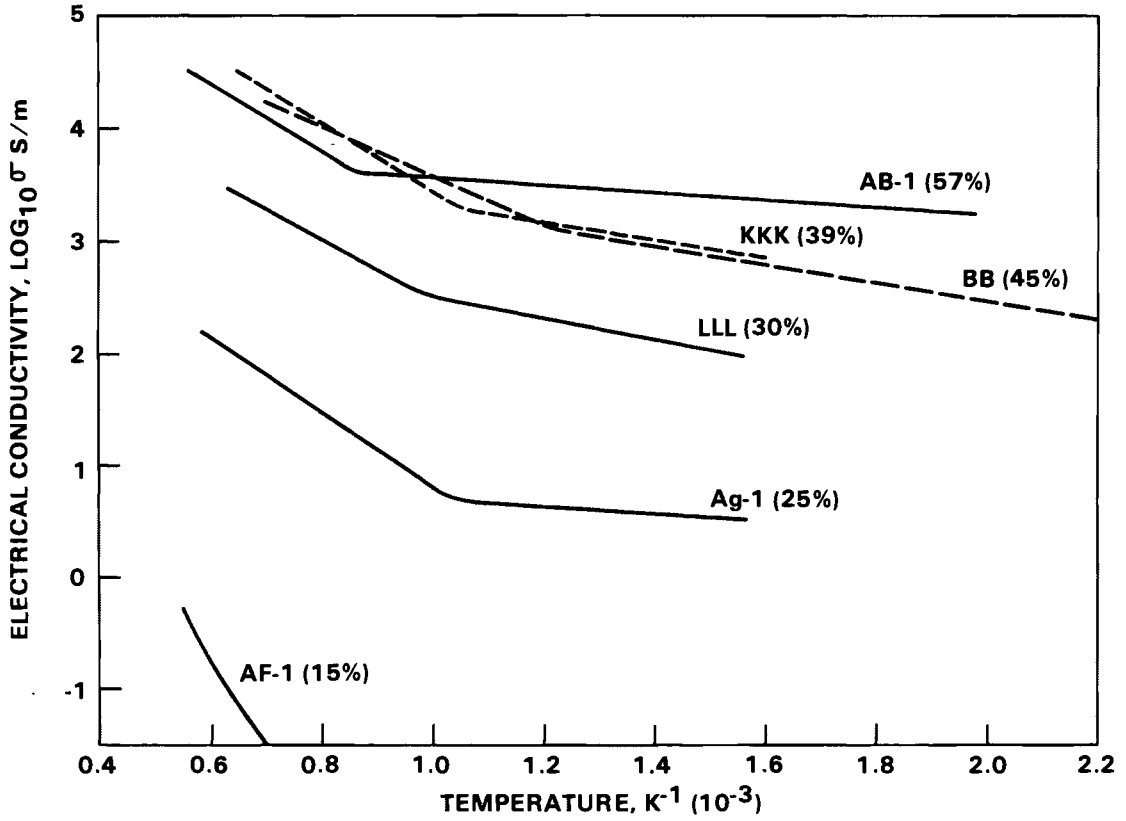

FIGURE 2. Electrical Conductivity of Several Hafnium Oxide-Rare Earth Oxide-Indium Oxide Compositions

Phase Equilibrium Studies

The binary phase diagrams of indium oxide-praseodymium oxide (In_2O_3-Pr_6O_{11}), indium oxide-zirconium oxide (In_2O_3-ZrO_2), indium oxide-hafnium oxide (In_2O_3-HfO_2) are being determined to identify the extent of the pyrochlore phase region. The Pr_2O_3-HfO_2 phase diagram has been reported previously (Kravchinskaya et al. 1978). Using these data, it is hoped that the HfO_2-In_2O_3-Pr_6O_{11} pseudoternary phase diagram can be developed and the compositions that exhibit the pyrochlore structures can be determined.

The binary phases are being determined by x-ray and metallographic examination of sintered compacts prepared by coprecipitation of the oxides that were then ball milled, cold pressed, and sintered. Sintering is at 1820K in air.

The phase diagram study of the In_2O_3-Pr_6O_{11}-HfO_2 system is continuing in order to determine the effects and limits of In_2O_3 on the $Pr_2Hf_2O_7$ phase. The results obtained from these phase equilibrium studies so far are summarized below:

In_2O_3-Pr_6O_{11}: The solubility of In_2O_3 in Pr_6O_{11} is less than 2 mol%. The solubility of Pr_6O_{11} in In_2O_3 is greater than 1 mol%, probably between 1 and 2 mol%. This solid solution has a_o values between 10.13 and 10.18 Å compared with In_2O_3 which is 10.12 Å. These oxides form an In_2O_3-Pr_6O_{11} single-phase compound with an orthorhombic structure with a,b,c, lattice constant values of 5.67, 5.92 and 8.17 Å, respectively. The solubility of In_2O_3 and Pr_6O_{11} in this compound has not been measured.

In_2O_3-ZrO_2: The solubility of In_2O_3 in ZrO_2 is 2 mol% with less than 3 mol% ZrO_2 solubility in In_2O_3. The fcc fluorite structure is stabilized between 7 and 15%, probably near 10 mol% with an a_o value near 5.46 Å. These results agree well with a previous study of the In_2O_3-ZrO_2 system (Schusterius and Padurow 1953), which also shows a fcc fluorite phase from 9 to 22 mol% In_2O_3, a limited solubility of ZrO_2 in In_2O_3, and a wide immiscibility between 22 and 93 mol% In_2O_3. However, the reported lattice constant value is 5.06 to 5.30 Å.

In_2O_3-HfO_2: The In_2O_3-HfO_2 phase diagram appears to be isomorphic to that of In_2O_3-ZrO_2 with the exception of an orthorhombic (a,b,c, = 5.03, 5.10, 5.18 Å) phase observed in conjunction with the fcc fluorite (a_o - 5.097 Å) phase near 40 mol% In_2O_3.

REFERENCES

Bates, J. L. and D. D. Marchant. 1982a. Development of Materials for Open Cycle MHD. Quarterly Report for the Period Ending March 1981. PNL-4001-1 Pacific Northwest Laboratory, Richland, Washington 1982.

Bates, J. L. and D. D. Marchant. 1982b. Development, Characterization and Evaluation of Materials for Open Cycle MHD. Quarterly Report for the Period Ending December 1980. PNL-2004-13, Pacific Northwest Laboratory, Richland, Washington.

Bates, J. L. and D. D. Marchant. 1983c. "Conducting Refractory Oxides for Molten Carbonate Fuel Cell Cathodes." Extended Abstracts. Fall Meeting of the Electro Chemical Society, October 17-21, 1982, Detroit, Michigan, p. 556.

Kravchinskaya, M. V., A. K. Kuznetsov, P. A. Tikhonov, and E. K. Koehler. 1978. "Phase Diagrams of the Systems HfO_2-Pr_2O_3 and Dy_2O_3-Pr_2O_3." Ceramurgia International 4(1).

Schusterius, C. and N. N. Padurow. 1953. "Relationships of Isomorphism in the System InO_3-Y_2O_3-ZrO_2." Ber. Deut. Ker. Ges. 30(10):235-239.

DISTRIBUTION

No. of Copies

OFFSITE

G. Rudins
Department of Energy
Mail Stop FE-22
Washington, DC 20545

M. Mintz
Department of Energy
Mail Stop FE-22
Washington, DC 20545

F. Marsik
Department of Energy
Mail Stop FE-22
Washington, DC 20545

J. Epstein
Department of Energy
Mail Stop FE-22
Washington, DC 20545

27 DOE Technical Information Center

C. Kolb
Aerodyne Research, Inc.
Center for Chemical and Environmental Physics
Bedford Research Park
Crosby Drive
Bedford, MA 91730

R. Cooper
Air Force Aero Propulsion Lab.
Aerospace Power Division
AFWAL/XRXP
Wright Patterson AFB, OH 45433

No. of Copies

J. Youngblood
Applied Technology Laboratory
P.O. Box 3809
Butte, MT 59701

T. Johnson
Argonne National Laboratory
9700 S. Cass Avenue
Argonne, IL 60439

M. Petrick
Argonne National Laboratory
9700 S. Cass Avenue
Argonne, IL 60439

C. Redman
Argonne National Laboratory
9700 S. Cass Avenue
Argonne, IL 60439

L. Whitehead
ARO, Inc.
AEDC Division
Arnold Air Force Station, TN 37389

F. Hals
AVCO Everett Research Laboratory
2385 Revere Beach Parkway
Everett, MA 02149

L. Nazzaro
Librarian
AVCO Everett Research Laboratory
2385 Revere Beach Parkway
Everett, MA 02149

S. Petty
AVCO Everett Research Laboratory
2385 Revere Beach Parkway
Everett, MA 02149

No. of Copies

R. Kessler
AVCO Everett Research Laboratory
2385 Revere Beach Parkway
Everett, MA 02149

A. C. Dolbec
Advanced Fossil Power Systems
Electric Power Research Institute
P.O. Box 10412
3412 Hillview Avenue
Palo Alto, CA 94303

P. Zieglebaum
Electric Power
Research Institute
P.O. Box 10412
3412 Hillview Avenue
Palo Alto, CA 94303

D. DeCoursin
FluiDyne Engineering Corp.
5900 Olson Memorial Highway
Minneapolis, MN 55422

J. Cutting
Gilbert Associates, Inc.
P.O. Box 1498
Reading, PA 19603

A. Dawson/NW14-2525
MIT/FBNML
170 Albany Street
Cambridge, MA 02139

B. Montgomery/MW14-3211
MIT/FBNML
170 Albany Street
Cambridge, MA 02139

H. K. Bowen
Massachusetts Institute of Technology
Department of Aeronautics and Astronautics
77 Massachusetts Avenue
Cambridge, MA 02139

No. of Copies

D. Murphree
Mississippi State University
Aerophysics and Aerospace Engineering
P.O. Drawer A/AP
Mississippi State, MS 29762

G. Staats
Mountain States Energy
Box 3767
Butte, MT 59701

R. Rosa
Department of Mechanical Engineering
Montana State University
Bozeman, MT 59715

G. Simmons
Multitech Inc.
P.O. Box 4078
Butte, MT 59701

M. Bloom
Polytechnic Institute of New York
Route 110
Farmingdale, NY 11735

R. Gibbons
Ralph M. Parsons Co.
100 West Walnut Street
Pasadena, CA 91124

R. Y. Pei
Rand Corporation
2100 M. Street NW
Washington, DC 20037

F. G. Blottner/1261
Sandia Laboratories
P.O. Box 500
Albuquerque, NM 87115

E. H. Eustis
Stanford University
Stanford, CA 94305

No. of
Copies

H. Koester
Stanford University
Stanford, CA 94305

S. Demetriades
STD Corporation
P.O. Box "C"
Arcadia, CA 91006

C. Maxwell
STD Corporation
P.O. Box "C"
Arcadia, CA 91006

H. Graham
TRW
One Space Park
Redondo Beach, CA 90278

J. Hardgrove
TRW
One Space Park
Redondo Beach, CA 90278

S. Schneider
U.S. Department of Commerce
National Bureau of Standards
Washington, DC 20234

T. Arrigoni
U.S. Department of Energy
Pittsburgh Energy Technology
Center
P.O. Box 10940
Pittsburgh, PA 15236

H. F. Chambers
U.S. Department of Energy
Pittsburgh Energy Technology
Center
P.O. Box 10940
Pittsburgh, PA 15236

No. of
Copies

S. Wu
Energy Conversion Division
University of Tennessee Space
Institute
Tullahoma, TN 37388

J. Chapman
Program Manager
University of Tennessee Space
Institute
Tullahoma, TN 37388

R. H. Smith
Section Manager
Planning and Information
Services
University of Tennessee Space
Institute
Tullahoma, TN 37388

W. Buckman
Westinghouse Electric
Corporation
Advanced Energy Systems Division
P.O. Box 10864
Pittsburgh, PA 15236

J. M. Feret
Westinghouse Electric
Corporation
Advanced Energy Systems Division
P.O. Box 10864
Pittsburgh, PA 15236

B. Rossing
Westinghouse Electric
Corporation
Research & Development Center
1310 Beulah Road
Pittsburgh, PA 15235

No. of Copies

FOREIGN

R. P. Indwar
Central Mine Planning & Design Institute, Ltd.
Gondwana Place
Kanke Rd.
Ranchi 834008 India

ONSITE

DOE Richland Operations Office

H. E. Ransom

No. of Copies

22 Pacific Northwest Laboratory

J. L. Bates (2)
P. E. Hart
D. D. Marchant (10)
C. R. Hann
R. P. Turcotte
Technical Information (5)
Publishing Coordination YO (2)